Catalysis Today 175 (2011) 435–441

Contents lists available at ScienceDirect

Catalysis Today

journal homepage: www.elsevier.com/locate/cattod

Etherification of 5-hydroxymethyl-2-furfural (HMF) with ethanol to biodiesel components using mesoporous solid acidic catalysts

P. Lanzafame[a,*], D.M. Temi[a], S. Perathoner[a], G. Centi[a], A. Macario[b], A. Aloise[b], G. Giordano[b]

[a] Department of Industrial Chemistry and Engineering of Materials and CASPE-INSTM, University of Messina, 98166 Messina, Italy
[b] Department of Chemical Engineering and Materials, University of Calabria, Rende, 87030 Cosenza, Italy

ARTICLE INFO

Article history:
Received 31 October 2010
Received in revised form 27 April 2011
Accepted 16 May 2011
Available online 16 June 2011

Keywords:
HMF
Biodiesel components
Acid sites
Mesoporous catalysts
Ethanol
Etherification

ABSTRACT

The etherification of 5-hydroxymethyl-2-furfural (HMF) with ethanol is studied over a series of mesoporous silica catalysts (Al-MCM-41 materials with different Si/Al ratio, and zirconia or sulfated zirconia supported over SBA-15) and compared with the behavior of H_2SO_4 and Amberlyst®15. The observed reaction products were 5-(ethoxymethyl)furan-2-carbaldehyde (EMF), 1,1-dietoxy ethane (DE) and ethyl 4-oxopentanoate (EOP). The selectivity to EMF and EOP is closely related to the presence of Lewis and/or Brønsted acidity on the catalyst, while the formation of DE is probably related to defect sites. The latter, being less reactive, catalyze the side reaction to DE only when strong Lewis and/or Brønsted acid sites are absent. Catalysts with only a strong Brønsted acidity react selectively to form EOP. When strong Lewis acid sites are present in the catalyst, e.g. by introducing ZrO_2 in SBA-15 or when extra-framework isolated Al^{3+} sites are present in the mesoporous channels, a high selectivity to EMF was observed. The results indicate that EMF, DE or EOP can be obtained selectively by direct reaction of HMF with bioethanol by tuning the acidity of the catalyst. EMF is a value biodiesel component, but the results also evidence the possibility to obtain selectively EOP in a one-step reaction, opening interesting perspectives to produce valeric biofuels by subsequent selective hydrogenation.

1. Introduction

5-Hydroxymethylfurfural (HMF) is formed as the main product in the acid-catalyzed conversion of ligno-cellulosic biowastes (residues of the agro-food production, municipal wastes, etc.) in industrial processes such as the Biofine®, but is also formed as byproduct in some pretreatments processes of cellulosic raw materials and should be removed due to its inhibition effect on the enzymatic fermentation. In addition, it is also the main reaction product in the novel conversion processes of ligno-cellulosic materials (straw, for example) using ionic liquids [1], an area of increasing interest. The valorization of HMF is thus of key relevance for the development of biorefineries [2], because it may be considered an excellent platform molecule which can be converted to energy products (2,5-dimethylfuran, an octane booster), monomers for high-value polymers (2,5-carboxyfuran and 2,5-hydroxymethylfuran) and valuable intermediates for fine chemistry.

While few recent papers discussed some of these reactions [3], no literature results have been reported on the relevant option to produce compounds for biodiesel, apart the general indication of the interest by Avantium, a spin-off company of Shell, in developing this kind of reaction compounds as part of the general class of new bio-based chemicals called "furanics" [4,5]. However, they have not given indications on the type of catalysts necessary and the reaction conditions, and thus essentially no literature data are available on this reaction.

The production of 2nd generation biodiesel from ligno-cellulosic sources is a commercial and strategic interest for Europe. Indeed about 60% of the new light cars are based on diesel engine but Europe needs to import both diesel and vegetable oils to produce 1st generation biodiesel (via transesterification of vegetable oils).

We report here for the first time the comparison of a series of mesoporous solid acid catalysts in the etherification of HMF by ethanol to produce a components for biodiesel and other valuable intermediate. The observed reaction products are 5-(ethoxymethyl)furan-2-carbaldehyde (EMF), 1,1-dietoxy ethane (DE) and ethyl 4-oxopentanoate (EOP). As reported by Avantium [4], EMF is an excellent additive for diesel, with high energy density of 8.7 kWh/L, similar to regular gasoline (8.8 kWh/L), nearly as good as diesel (9.7 kWh/L) and significantly higher than ethanol (6.1 kWh/L). Blends with regular diesel yielded positive results with a significant reduction of soot (fine particulates), and a reduction of the SO_x emissions. EOP, after hydrogenation, gives valeric ester, a biofuel developed by researchers at Shell Global Solutions, although through a different route: via levulinic acid, converted to

* Corresponding author.
E-mail address: planzafame@ingegneria.unime.it (P. Lanzafame).

0920-5861/$ – see front matter © 2011 Elsevier B.V. All rights reserved.
doi:10.1016/j.cattod.2011.05.008

Table 1
Textural characteristic of the mesoporous catalysts.

Catalyst	Si/Al ratio	BET surface area (m^2/g)	Total pore volume (cm^3/g)	Average channel diameter (Å)
SBA-15	>1000	763	0.94	51.2
Z-SBA-15	>1000	469	0.69	48.8
SZ-SBA-15	>1000	426	0.61	44.7
Al-MCM-41 (25)	25	1306	0.97	39.5
Al-MCM-41 (50)	50	1210	0.92	37.8
Al-MCM-41 (75)	75	1160	0.85	34.2

gamma-valerolactone, which is hydrogenated to valeric acid and then esterified to produce valerate esters [6]. Depending on the reactants used in the esterification, valeric biofuels may be in the form of biogasoline or biodiesel, and can be well mixed with other fuels currently available. In a mixture with 15% valeric biofuels, road tests for over 250,000 km, did not show negative impacts in the motor, tank, or fuel lines, and excellent performances. The selective hydrogenation of the chetonic group in beta position of EOP may thus also form valuable biofuels, with an alternative route to that proposed and patented by Shell [6,7]. Valerate esters, such as ethyl valerate (also called ethyl pentanoate), are esters also commonly used in fragrance and flavouring applications. Their uses as fuel additives also suppress the unpleasant odor characteristic of the fuel produced during incomplete combustion and are also added to decrease the vapor pressure of gasoline.

DE (better known as acetal) is also a potentially valuable additive for biofuels. When this compound is blended into diesel, minor influences on fuel properties are observed. Only a small decrease in the heating value, distillation and flashpoint are noticed, but the net effect was a reduction in the emission of CO_2 for European stationary cycle [8–10]. The addition of the acetal leads also to a marked decrease in particle number emissions, although an increase in acetaldehyde emissions. Therefore, all the different reaction products observed in the reaction of HMF with ethanol over mesoporous acid catalysts are valuable to produce biofuels or other interesting chemicals.

Different acidic catalysts, such as silico-aluminates, zeolites or resins [11,12] are reported to be active in the etherification reaction (of different substrates), but when the substrate is a substituted heterocyclic molecule as in our case (HMF), diffusional problems can be present in zeolites and other microporous materials due to the bulky dimension of the products. In order to overcome these limitations, we have focused the study on mesoporous materials (MCM-41 and SBA-15) which present high surface area, diameter of the channels in the range of 3–10 nm (depending of the preparation conditions) and a high thermal and hydrothermal stability. The acidity of these catalysts can be tuned by introducing aluminum or oxides of transition metals into the mesoporous structure.

Three Al-containing mesoporous silica samples (Al-MCM-41 with different Si/Al ratios) were prepared and tested, in order to have a screening of the role of acidity on the etherification of HMF by ethanol. Furthermore, in order to discuss the effect of the presence of Lewis acidity, ZrO_2 supported over mesoporous silica was also prepared and tested, because both Brønsted (protonic) and Lewis (aprotic) acidic centres exist at the surface of zirconia [13]. Being known that after sulfation of zirconia, there is a decrease of the Lewis acidity and an increase of the Brønsted acidity [13], we have tested also the sample after sulfation. Zirconia was supported over the mesoporous silica, in order to have high oxide dispersion and samples more comparable with the Al-MCM-41 series. However, SBA-15 type mesoporous silica instead that MCM-41 was used, because the slightly larger dimensions of the channels allows obtaining a better dispersion of zirconia. Finally, in order to complete the screening, a homogeneous acid catalyst (H_2SO_4) and an alternative strong-acid heterogeneous resin-type catalyst (Amberlyst®15) were also evaluated.

2. Experimental

2.1. Reactants

The silica source used for preparation of MCM-41 based catalysts was the fumed silica (Aldrich). The structure directing agent used was cetyltrimethylammonium bromide (CTABr, 98% Aldrich), sodium hydroxide (97%, Carlo Erba) was used as mineralizing agent and sodium aluminate ($NaAlO_2$, 99%, Carlo Erba) was used as aluminum source.

The reactants used for the preparation of SBA-15 based catalysts were tetraethyl orthosilicate (TEOS, 99.999% Aldrich) as silica source, Pluronic P123 triblock polymer (PEO-PPO-PEO, Aldrich) as directing agent and zirconium(IV) oxychlorideoctahydrate (≥99.5%, Sigma–Aldrich) as zirconia source. 5-Hydroxymethyl-2-furfural (≥99%, Aldrich), Ethanol (≥99.8%, Fluka) were used for the catalytic etherification reaction.

2.2. Catalysts preparation

2.2.1. Preparation of MCM-41 type catalysts

MCM-41 materials, with different Si/Al ratios, were synthesized starting from the following molar gel composition:

$$1SiO_2–0.18Na_2O–0.2CTABr–xAl_2O_3–40H_2O$$

where x ranges from 0.0067 to 0.02. The procedure adopted to synthesize the Al-MCM-41 materials consisted in the dissolution of the structure directing agent in distilled water that was followed by addition of a hydroxide solution and, finally, by addition of aluminum and silica sources. The crystallization time and temperature were respectively of 48 h and 140 °C. The exact Si/Al molar ratio used in the starting synthesis gel of different mesoporous materials is reported in Table 1.

The solid products, obtained by vacuum filtration, were then washed with distilled water and dried at 100 °C. All mesoporous materials were calcined at 550 °C in flow of air for 8 h. In order to obtain the catalysts in the H-form, the samples were ion-exchanged by an ammonium salt [14] after the calcinations procedure and then further annealed at 450 °C.

2.2.2. Preparation of SBA-15 type catalysts

Mesoporous SBA-15 was prepared according to literature and the detailed procedure described elsewhere [15]. ZrO_2 was dispersed on the SBA-15 support by an urea hydrolysis method using zirconium(IV) oxychloride ($ZrOCl_2·8H_2O$) as zirconia source [16]. The theoretical zirconia loading was 30 wt%. The mixture was refluxed at 90 °C for 5 h (pH about 8), and the resulting gel was filtered and washed with distilled water until removal of chloride. After centrifugation, the ZrO_2-SBA-15 gel was dried and calcined at 550 °C for 6 h. This sample is indicated hereinafter as Z-SBA-15. Z-SBA-15 was sulfated using H_2SO_4 1 N (15 ml/g) at room temperature, dried and calcined at 550 °C for 3 h. This catalysts is indicated hereinafter as SZ-SBA-15.

2.3. Catalysts characterization

Powder X-ray diffraction (XRD) data were recorded using a Phillips PW 1710 diffractometer with Cu Kα radiation. The samples were scanned in the range of 2θ from 1 to 8° in steps of 0.005° with a count time of 1 s at each point.

BET surface area and physical properties of samples were evaluated by N_2 adsorption/desorption isotherms carried out at 77 K on a Micromeritics ASAP 2020 sorption analyser. The specific surface area was determined by applying the BET equation to the isotherm. Mesopore size distribution was calculated using the adsorption branch of the nitrogen adsorption isotherm and the Barrett–Joyner–Halenda (BJH) formula. The average pore diameter and the cumulative volume were obtained from the distribution curve of the mesopore sizes.

The morphology and habit of the crystalline phase of the products were examined by scanning electron microscope (SEM, JEOL JSTM 330 A). The chemical composition of the crystals was determined by energy dispersive X-ray analysis (EDX).

^{29}Si MAS-NMR spectra were recorded on a Bruker MSL 400 or a Bruker CXP 200 spectrometer. For ^{29}Si (39.7 MHz) a 6 μs ($\theta = \pi/6$) pulse was used with a repetition time of 6 s. A repetition time of 60 s led to a spectrum that was identical to the one obtained with a 6 s repetition time [17].

For the FTIR measurements, the calcined samples were pressed into thin, self-supporting wafer (surface density about 20 mg cm^{-2}) and the spectra were collected, at a resolution of 2 cm^{-1} on a PerkinElmer FTIR spectrophotometer equipped with a MCT detector. The self-supporting wafers were prepared and activated under dynamic vacuum (10^{-4} Torr) for 1 h at 573 K, in an IR cell allowing in situ thermal treatments, gas dosage (CO) and IR measurements to be carried out both at room temperature and at a nominal temperature of 77 K, presumably in fact around 100 K. Difference spectra are obtained after subtraction of the spectrum of the naked sample.

2.4. Catalytic experiments

The catalytic etherification of HMF with ethanol was carried out in a Parr autoclave reactor (Teflon-lined) provided with Parr 4848 controller. Reaction tests were carried out at 140 °C for 5 h under autogeneous pressure. As a general procedure, 2.5 mmol HMF were dissolved in 3.4 ml of ethanol and put in the reactor containing the catalyst. The mixture was stirred at ca. 1500 rpm, and the progress of the reaction was followed by taking samples at regular periods and analyzed by Finnigan GC–MS.

3. Results

3.1. Low-angle X-ray diffraction

Three characteristic diffraction lines of SBA-15 structure, (1 0 0), (1 1 0) and (2 0 0) at ca. $2\theta = 0.95$, 1.6, 1.95, respectively, which are characteristic of *P6mm* hexagonal mesoporous materials, were observed in the low-angle X-ray patterns (Fig. 1). The XRD pattern of ZrO_2-SBA-15 is qualitatively similar to that of SBA-15, but a weakening and broadening of the (1 0 0), (1 1 0) and (2 0 0) reflections is observed which also shift to slightly higher angles. This indicates a lower degree of order in ZrO_2-SBA-15 with respect to SBA-15 as well as a slightly different 2D packing, but this is usually observed when an oxide is loaded onto mesoporous silica [18].

At higher angles, no further diffraction lines were detected, indicating that crystalline ZrO_2 is not present, confirming that the preparation leads to a high dispersion of zirconia on the mesoporous silica support.

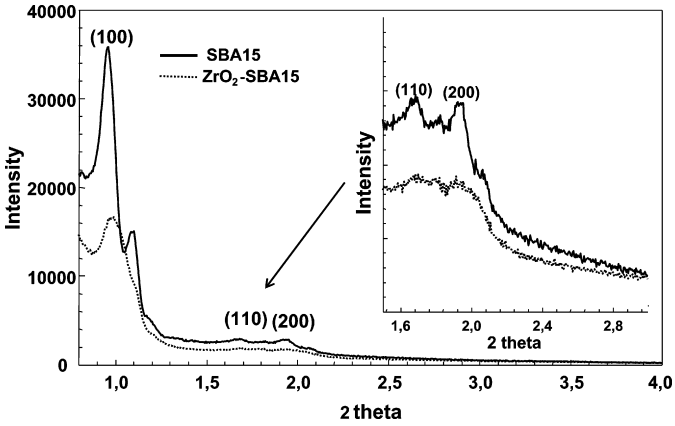

Fig. 1. Low-angle X-ray scattering of SBA-15 based catalysts: SBA-15 and ZrO_2-SBA-15.

Low-angle X-ray diffraction pattern for a typical MCM-41 sample shows four well-resolved peaks that can be indexed as (1 0 0), (1 1 0), (2 0 0) and (2 1 0) reflections associated with the hexagonal symmetry. The XRD results of the prepared MCM-41 based catalysts show an intense diffraction peak at $2\theta = 2.5°$ and three, not well resolved peaks in the range of 2θ from 3.5 to 5.5, suggesting that a minor degree of structural ordering was obtained.

3.2. Porosity characterization

Nitrogen adsorption analysis was made on the prepared samples and the main results are summarized in Table 1. For all samples, the isotherms of nitrogen adsorption show the typical IV-type profile, according to the IUPAC classification, consisting in a step condensation behavior due to mesopores. Table 1 reports the specific surface area and the total pore volume for all samples evidencing that these parameters decrease from 1306 to 1160 m^2/g and 0.97 to 0.85 cm^3/g, respectively, when the Si/Al ratio is increased from 25 to 75 in the MCM-41 based samples. In the SBA-15 based samples, a decrease of the pore diameter is observed after the addition of the zirconia suggesting that the oxide is mainly located inside the pores of the SBA-15.

3.3. Electron microscopy characterization

SEM micrographs of SBA-15 based samples shows the typical SBA-15 wheat-like morphology with a crystal size in the range of 1–2 μm. A well homogeneous distribution of zirconia, without detection of Zr-rich areas, was evidenced by EDX measurements.

The homogeneity of the distribution of zirconium and its influence on the well-ordered hexagonal array of mesopores typical of SBA-15 were also analyzed by transmission electron microscopy (TEM). No evidences were observed of the presence of zirconia crystallites on the outer surface of the mesoporous silica, confirming thus that XRD and SEM indications that zirconia is mainly located within the mesoporous silica channels as an XRD-amorphous phase, probably homogeneously distributed on the inner walls of the channels, in agreement with textural data. TEM of the parent SBA-15 shows an homogeneous ordering of channels and it evidences that the diameter of the channels is about 6.4 nm, with a wall thickness of about 3 nm.

The SEM images of the Al-MCM-41 samples indicate agglomerates with sizes between 4 and 200 μm, but they did not show a tendency to form particles with a particular morphology.

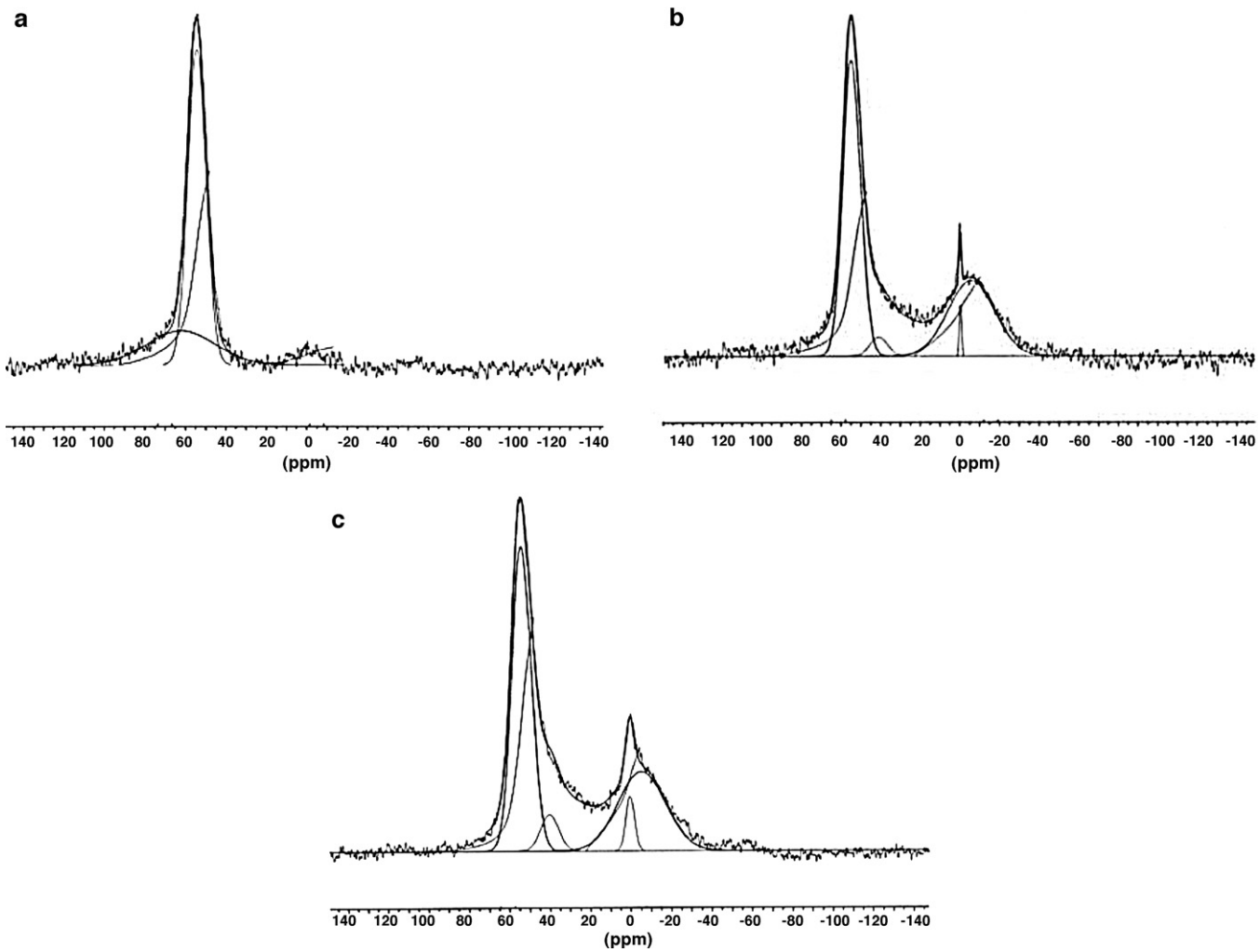

Fig. 2. ^{27}Al NMR of the samples Al-MCM-41 (25) (a), Al-MCM-41 (50) (b) and Al-MCM-41 (75) (c).

3.4. NMR

The ^{27}Al MAS and ^{29}Si MAS NMR spectra were registered on all Al-MCM-41 samples after calcinations in order to evidence the typology of acidic sites.

Fig. 2 show the ^{27}Al-NMR spectra of the Al-MCM-41 samples after calcination. The NMR line at ca. 54 ppm can be assigned to the four-coordinate structural aluminum [$Al^{(-)}(OSi)_4$]. Increasing the amount of the aluminum in the starting synthesis gel, from the sample Al-MCM-41 (75) to the sample Al-MCM-41 (25), new NMR lines are detected. These lines are at ca. 40, 0 and −6 ppm and can be ascribed to the aluminum in octahedral coordination: at 0 for the aluminum hexa-hydrated [$Al(H_2O)_6^{3+}$], at −6 ppm, for [$Al(OSi)_4(OH)_2$] and at 40 ppm for the five-coordinated aluminum [19].

The presence of these NMR lines clearly show that, increasing the aluminum content in the starting synthesis gel, the extra-framework aluminum increases too.

While, the aluminum intra-framework increases only when the Al-MCM-41 sample preparation starts from a Si/Al synthesis gel ratio equal or higher than 50.

In Tables 2 and 3 the results of the quantitative analysis carried out on the ^{27}Al-NMR and ^{29}Si-NMR spectra of the calcined Al-MCM-41 samples, are reported. From these results it is possible to confirm that almost the totality of the aluminum present in the Al-MCM-41 (75) is intra-framework.

It is possible to observe that, for the sample Al-MCM-41 (50) and Al-MCM-41 (75) the defective sites and the intra-framework aluminum content are almost the same. While for the sample Al-MCM-41 (25) the amount of the SiOAl groups (aluminum intra-

Table 2
^{27}Al MAS NMR for calcined Al-MCM-41 materials.

Sample	Si/Al[a] in the solid	Al/(Al + Si) [%]	$Al^{(-)}(OSi)_4$ [%]	$Al^{(-)}(OSi)_3OH$ [%]	Aluminum extra-framework [%]	
			δ = 54 ppm	δ = 40 ppm	δ = 0 ppm	δ = −6 ppm
Al-MCM-41 (25)	21	4.6	37	36	3	24
Al-MCM-41 (50)	39	2.5	39	34	1	26
Al-MCM-41 (75)	38	2.6	95	–	–	5

[a] Si/Al ratio calculated by EDX analysis carried out on a sample layer lower than 1 μm.

Table 3
^{29}Si MAS NMR for calcined Al-MCM-41 materials.

Sample	$Si(OH)_2$ $\delta = -92$ ppm [%]	$\delta = -100$ ppm [%] SiOH + SiOAl		$Si(OSi)_4$ $\delta = -109$ ppm [%]
Al-MCM-41 (25)	6	21	18	55
Al-MCM-41 (50)	7	25	10	58
Al-MCM-41 (75)	6	28	10	56

framework) strongly increases, indicating a higher Brønsted acidity of this sample, with respect to the samples with a lower amount of aluminum in their structure (Al-MCM-41 (50) and Al-MCM-41 (75) samples). Simultaneously, from the results reported in Table 2, it is also possible to affirm that increasing the extra-framework aluminum content, the amount of Lewis acid sites increases too.

Comparing the samples Al-MCM-41 (25) and Al-MCM-41 (50) it is possible to claim that they have almost the same intensity of Lewis acid sites but the Al-MCM-41 (25) possess also a higher Brønsted acidity. Finally for the Al-MCM-41 (75) sample, only a Brønsted acidity can be detected on its surface.

Finally, comparing again the samples Al-MCM-41 (50) and Al-MCM-41 (75), it is possible to affirm that the Brønsted acidity for these samples is almost the same but for the sample Al-MCM-41 (50) the Lewis acid sites are also present in its surface.

This different surface acidity of the mesoporous materials can strongly affect their catalytic behavior in the HMF etherification.

3.5. Infrared characterization

The analysis of the IR spectra for the Al-MCM-41 (50) sample (Fig. 3) evidences abroad band at 3740 cm^{-1}, assigned to isolated Si–OH groups, and indicating the presence of a high number of defects in the MCM-41 structure, in agreement with NMR analysis.

The IR spectra after adsorption of CO at low temperature (77 K) on Al-MCM-41 sample are shown in Fig. 4. The spectra relate to the adsorption of increasing amounts of CO (equilibrium pressures: 0.08–2.5 mbar) in the CO stretching region (2250–2050 cm^{-1}). At low coverage (curve 1), two absorptions are present at 2230 and 2176 cm^{-1}, the latter accompanied by a tailing at 2170–2160 cm^{-1}. At higher coverage (curves 2–5), the component at 2176 cm^{-1} shifts to lower frequencies (2172 cm^{-1}) and a band increases at 2157 cm^{-1}, due to CO interacting via H-bonding with silanols, followed by a complex absorption at about 2138 cm^{-1} assigned to physisorbed CO (liquid-like). Two Al^{3+} species have been observed to exist in other Al-containing MCM-41 materials [20], responsible for CO absorptions at the same frequencies discussed above. The stronger one, absorbing at 2230 cm^{-1}, was attributed to extraframework Al sites. The weaker one, absorbing at 2176–2172 cm^{-1}, has been assigned [20] to $Al(OSi)_3$ species located in the amorphous structure of the silica walls.

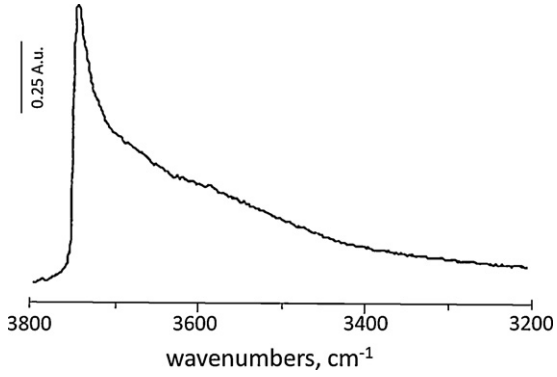

Fig. 3. FTIR spectra of Al-MCM-41 (50) after degassing at 550 °C.

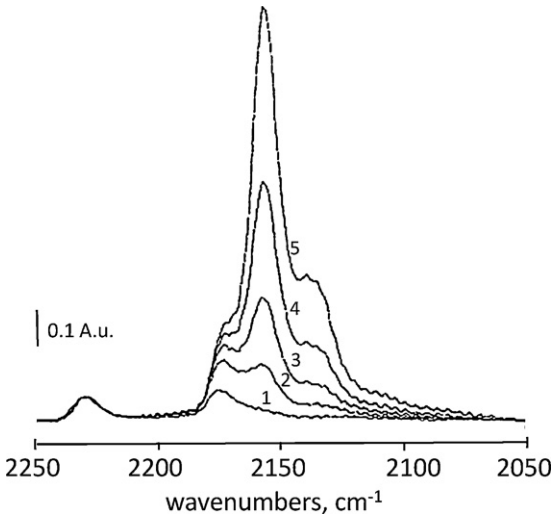

Fig. 4. FTIR spectra of Al-MCM-41 (50) after CO absorption at low temperature.

3.6. Catalytic activity

The prepared mesoporous catalysts were studied in the etherification of HMF with ethanol to obtain the biodiesel component EMF, and compared with the performances of the reference H_2SO_4 and Amberlyst®15 catalysts. The results are summarized in Table 4. Together with the desiderate ether (EMF), other reaction products were detected: 1,1-dietoxy ethane (DE) and ethyl 4-oxopentanoate (EOP). The formation of these products depends considerably on the nature of the catalyst.

The use of a homogeneous acid (H_2SO_4) gives rise to the selective formation of EOP instead of EMF, with complete conversion of HMF and formation of EMF only in low amounts. Using a heterogeneous strong acid catalyst such as Amberlyst®15 a complete conversion of HMF to EOP is also observed, with even higher selectivity to EOP with respect to the homogeneous acid catalyst. On the contrary, at the same reaction temperature (140 °C) without the addition of an acid or an acidic solid catalyst the conversion of HMF was close to zero. Temperature plays an important role in this reaction. H_2SO_4 at 100 °C gives a very low conversion of HMF with only traces of the desired products.

The catalytic behavior of the Al-MCM-41 samples is quite different from that of the strong acid catalysts discussed before. For these catalysts, a high conversion of HMF (except in the case of Al-MCM-41 (75)) can be observed, but EMF and DE were obtained in addition to the EOP. No formation of EMF and EOP can be observed

Table 4
Catalytic results of the performances of the acidic catalysts in the etherification of HMF with ethanol at 140 °C. See Section 2 for the other reaction conditions.

Catalyst	HMF conversion (%)	EMF yield (%)	EOP yield (%)	DE yield (%)
SBA-15	75	–	–	54
Z-SBA-15	100	76	23	–
SZ-SBA-15	100	62	35	–
Al-MCM-41 (25)	100	37	47	12
Al-MCM-41 (50)	100	68	10	13
Al-MCM-41 (75)	61	–	–	19
Amberlyst®15	100	–	>99	–
H_2SO_4	100	3	96	–

HMF: 5-hydroxymethylfurfural; EMF: 5-(ethoxymethyl)furan-2-carbaldehyde; EOP: ethyl 4-oxopentanoate; DE: 1,1-dietoxy ethane.

using the catalyst Al-MCM-41 (75), and only DE as reaction product was observed with a yield of about 20%. The conversion of HMF is also low, but higher than expected if only DE forms. No other products of reaction were detected, apart from some formaldehyde. Thus probably for this sample some heavier products which remain on the catalyst may form. The carbon balance in the other samples was instead typically close to 100%, apart for the SBA-15 mesoporous silica, which also shows the formation of only DE as the reaction product, but with a yield lower than expected from HMF conversion. Therefore, both the samples showing the weaker acidity (Al-MCM-41 (75) and SBA-15) have a similar behavior: lower HMF conversion, DE as the main detected reaction product, and defect in the carbon balance indicating the probable formation of heavier reaction products.

On increasing the Al content in the Al-MCM-41 series, the amount of DE decreases slightly, the amount of EOP increases significantly becoming the main reaction product in Al-MCM-41 (25), while the formation of the aimed product (EMF) passes through a maximum.

In the case of zirconia supported over mesoporous silica, higher selectivity to EMF is observed, while the formation of DE is absent. The use of sulfated zirconia with respect to not-sulfated one determines a lowering in the EMF yield, and a corresponding increase in the yield of EOP. The mesoporous parent silica, e.g. without zirconia, shows a lower activity in HMF conversion, and only the formation of DE.

4. Discussion

4.1. Reaction pathways

The main reaction network of the studied reaction is summarized in Scheme 1. In addition, to the aimed biodiesel component EMF, other products of interest for biodiesel and in general biofuel production, such as EOP and DE were obtained, apparently in parallel reactions.

Table 4 evidences the considerable effect on the selectivity induced from the change of the acid properties of the mesoporous catalyst.

Although no study on the reaction mechanism was made, the formation of EMF can be easily explained with the well-known mechanism of nucleophilic attack of ethanol on the oxonium ion generated by interaction between the acidic sites on the catalyst and the hydroxylic group on the HMF. The formation of EOP is instead coherent with the acid catalyzed degradation mechanism of HMF to levulinc acid [21] and the subsequent esterification reaction with ethanol to give the corresponding ester (EOP). This pathway is quite interesting because it could allow to obtain directly valerate ester in a one pot reaction by direct hydrogenation of obtained EOP.

The formation of DE, although always associated to a moderate conversion of HMF, can be not understood through a reaction between HMF and ethanol, but it is probably due to the reaction between ethanol and the small amount of acetaldehyde in equilibrium with it [22]. HMF could be converted to products not detectable in our analytical conditions. However, the study on the mechanism and the conditions of this pathway should be investigated more in detail, considering the possible use of DE as diesel fuel additive.

4.2. Role of the catalysts acidity

The remarkable influence of the catalyst characteristics on the etherification of HMF (Table 4) can be rationalized in terms of Lewis and/or Brønsted acidity properties of the catalysts. The high selectivity to EOP showed by H_2SO_4 and Amberlyst®15 is clearly associated to the presence of strong Brønsted acidity that promotes the degradation of HMF to levulinic acid (further then converted to the ester), as discussed before. This result is also confirmed by the data obtained using the MCM-41 based catalysts: when the Brønsted acid sites strength on MCM-41 increases by introduction of aluminum species in the framework (wall) of the mesoporous structure (Al-MCM-41 (25)), EOP is the main product even if EMF is also formed. In the sample with a lower Si/Al ratio (Al-MCM-41 (50)), e.g. decreasing the amount of strong Brønsted acid sites, the etherification of HMF to EMF is favored with respect to the degradation reaction to EOP. Therefore, the EOP yield significantly decreases with a parallel increase in EMF yield. As discussed below, the formation of EMF is probably associated with the presence of Lewis acid sites, due to extra-framework (isolated) Al^{3+} ions. FTIR characterization (Fig. 4) confirms the presence of this type of sites. Increasing the amount of Al in Al-MCM-41, increases the amount of strong Brønsted acid sites, while probably isolated Al^{3+} extra-framework sites tend to aggregate forming polymeric Al-(hydr)oxide nanoparticles which do not show Lewis acidity. Consistently, the formation of EMF decreases and significantly increases the EOP yield.

The low acidity of Al-MCM-41 (75) catalyst is probably not enough to activate the substrate to the degradation, and due to the low amount of Al ions, Al^{3+} extra-framework sites were not detected. Therefore, this sample results also inactive for the etherification of HMF. DE, deriving possibly from side reactions of ethanol, is the only detectable product in low amounts. Note that the formation of this product is probably also favored by the catalyst, because for other samples (zirconia on mesoporous silica, Amberlyst®15 and H_2SO_4) it is not detected. NMR data (Tables 2 and 3) indicate that the MCM-41 is highly defective, due to the presence of hydroxyl nests. Probably these sites or traces of other transition metals such as iron present as impurities introduced during the preparation catalyze the oxidation of ethanol to acetaldehyde, which is the critical step for acetal (DE) formation. However, these sites are also reasonably associated to slow side reactions responsible for the conversion of HMF to undetected (probably heavier) products. The mechanism should be better clarified, but being present only in the less reactive and selective samples, it is of minor interest.

The role of Lewis acidity in EMF synthesis is further demonstrated from the performances of zirconia supported over mesoporous silica. The parent sample (SBA-15) shows only very weak acidity associated to the silanol group present in the inner walls on the channels of SBA-15. The behavior is analogous to the Al-MCM-41 (75). The introduction of ZrO_2 determines an increase of the Lewis acidity, associated to the surface exposed Zr^{4+} ions of XRD not detectable zirconia (amorphous or nanocrystalline) well dispersed in the mesoporous silica (SBA-15). Electron micrograph characterization, XRD and porosity measurements confirm the good dispersion of the zirconia. It is known that zirconia supported over silica shows both strong Lewis and Brønsted acidity [23], and it is reasonable that the number of Lewis acid sites is higher with respect to the limited amount of extra-framework Al^{3+} ions in Al-MCM-41. It is thus well consistent that Z-SBA-15 shows a higher formation of the desired compound (EMF) together with less amounts of EOP. By supporting the zirconia, the defect sites present in the parent mesoporous silica are suppressed and thus the formation of DE is inhibited.

As mentioned above, the sulfation of zirconia decreases the Lewis acidity and increases the Brønsted acidity [13]. Consistently, we observed that the yield in EOP on SZ-SBA-15 is higher with respect to Z-SBA-15, while the yield in EMF decreases in parallel.

The adsorption of HMF on the Lewis acidic sites forms probably the oxonium ion and EMF is then obtained by the nucleophilic attack of the ethanol. The presence of Lewis acidity is therefore critical to address the reaction towards the etherification of HMF

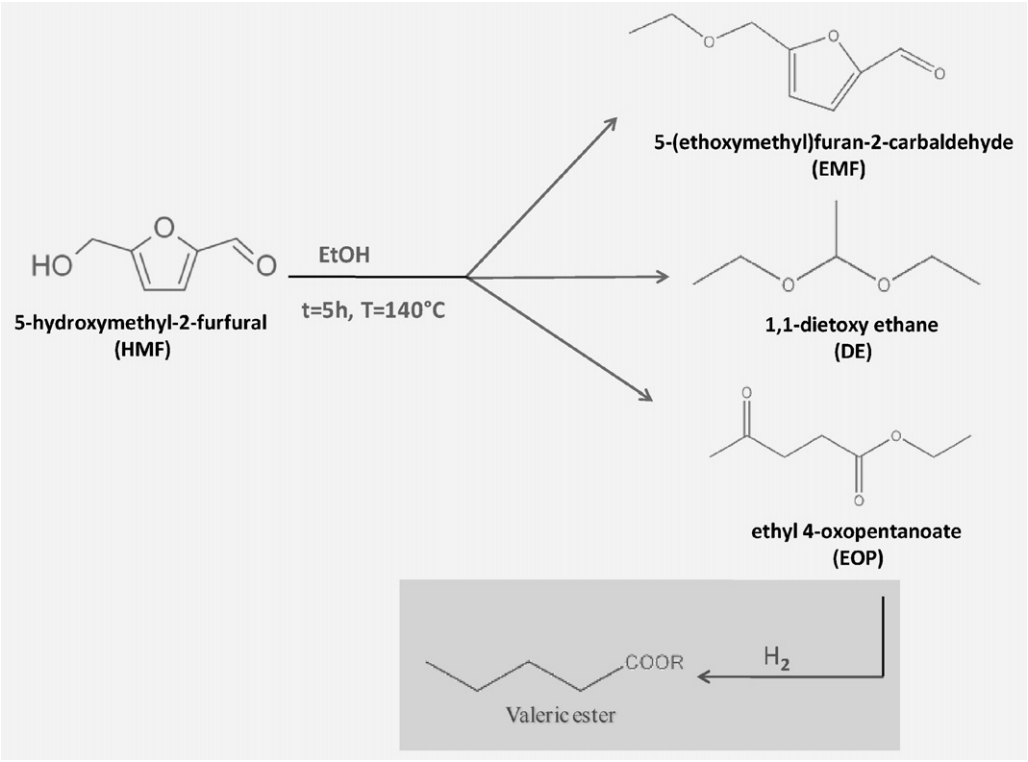

Scheme 1. General reaction network in the etherification of HMF with ethanol over mesoporous acid catalysts.

to EMF. Further studies are necessary for a better understanding of the reaction network and the role of the acidity of the catalyst, but present data already indicate how the selectivity in the etherification of HMF with ethanol can be tuned towards different products. All the obtained products are of interest for the production of biofuels, and it was thus demonstrated that by controlling the acid properties of the catalysts, and the presence of defect sites as well, it is possible to produce different valuable biofuel components in this reaction of relevant interest for the development of novel and clean catalytic routes in biorefineries.

5. Conclusions

The data reported here indicate that acidic catalysts convert HMF to EMF and other valuable intermediate, such as DE and EOP with high yields. The selectivity to EMF and EOP is closely related to the presence of Lewis and/or Brønsted acidity on the catalyst, while the formation of DE is probably related to defect sites. The latter, being less reactive, catalyze the side reaction to DE only when strong Lewis and/or Brønsted acid sites are absent. Catalysts like H_2SO_4, Amberlyst®15 and Al-MCM-41 (25), characterized from a strong Brønsted acidity, favor the formation of EOP. When strong Lewis acid sites are present in the catalyst, e.g. by introducing ZrO_2 in SBA-15 (Z-SBA-15) or when extra-framework isolated Al^{3+} sites are present such as in Al-MCM-41 (50), a higher selectivity to EMF is observed. Weaker acidic catalysts, like as Al-MCM-41 (75) and pure SBA-15, form DE as the main reaction product, albeit HMF partially convert to undetected products.

The results presented here allow thus to conclude that EMF, DE or EOP can be obtained selectively by direct reaction of HMF with bioethanol by tuning the acidity of the catalyst. EMF is a value biodiesel component, but the results also evidence the possibility to obtain selectively EOP in one-step reaction, opening interesting perspectives to produce valeric biofuels (valerate esters) by subsequent selective hydrogenation.

Acknowledgements

This lecture is realized in the frame of the activities of the PRIN08 project “Catalytic upgrading of the fraction C5 in ligno-cellulosic biorefineries” and the COST Action CM0903 “Utilisation of biomass for fuel and Chemicals (UBIOCHEM)”.

References

[1] J.B. Binder, R.T. Raines, J. Am. Chem. Soc. 131 (2009) 1979.
[2] G. Centi, R.A. van Santen, Catalysis for Renewables, Wiley-VCG, Weinheim, Germany, 2007.
[3] M. Mascal, E.B. Nikitin, Angew. Chem. Int. Ed. 47 (2008) 7924.
[4] P. Imhof, A.S. Dias, E. de Jong, G.-J. Gruter, Presented at 21th NAM S. Francisco, US, June 2009, p. OA02.
[5] G.J.M. Gruter, F. Dautzenberg, Eur. Patent EP 1834950 (2007).
[6] J.P. Lange, R. Price, P.M. Ayoub, J. Louis, L. Petrus, L. Clarke, H. Gosselink, Angew. Chem. Int. Ed. 49 (2010) 4479.
[7] L. Clarke, A. Felix-Moore, J.J.J. Louis, J. Smith, PCT Int. Appl., WO 2010000761 (2010).
[8] A. Bertola, K. Boulouchos, SAE Techn. paper 01-2885 (2000).
[9] M. Natarajan, M.A. Gonzalez, E.A. Frame, D.W. Naegeli, E. Liney, T. Asmus, P. Piel, W. Clark, J.P. Wallace, J. Garbak, SAE Techn. paper 01-3631 (2001).
[10] K.E. Nord, D. Haupt, Environ. Sci. Technol. 39 (16) (2005) 6260.
[11] P. Berteau, S. Ceckiewicz, B. Delmon, Appl. Catal. 31 (1987) 361.
[12] F. Collignon, R. Loender, J.A. Martens, P.A. Jacobs, G. Poncelet, J. Catal. 182 (1999) 302.
[13] C. Morterra, G. Cerrato, V. Bolis, Catal. Today 17 (3) (1993) 505.
[14] M. Kitamura, H. Hichihashi, I. Tojima, US Patent 5,212,302 (1993).
[15] P. Lanzafame, S. Perathoner, G. Centi, F. Frusteri, J. Porous Mater. 14 (2007) 305.
[16] S Garg, K. Soni, G.M. Kumaran, R. Bal, K. Gora-Marek, J.K. Gupta, L.D. Sharma, G.M. Dhar, Catal. Today 141 (2009) 125.
[17] P. Sutra, F. Fajula, D. Brunel, P. Lentz, G. Daelen, J.B. Nagy, Colloids Surf. A 158 (1999) 21.
[18] S. Perathoner, P. Lanzafame, R. Passalacqua, G. Centi, R. Schlögl, D.S. Su, Micropor. Mesopor. Mater. 90 (1–3) (2006) 347.
[19] G. Engelhardt, D. Michel, High-Resolution Solid-state of Silicates and Zeolites, John Wiley & Sons, Chichester, 1987.
[20] B. Bonelli, M.F. Ribeiro, A.P. Antunes, S. Valange, Z. Gabelica, E. Garrone, Micropor. Mesopor. Mater. 54 (3) (2002) 305.
[21] J. Horvat, B. Klaić, B. Metelko, V. Šunjić, Tetrahedron Lett. 26 (1985) 2111.
[22] M.F. Gomez, L.A. Arrúa, M.C. Abello, React. Kinet. Catal. Lett. 73 (2001) 143.
[23] Y. Wang, J. Ma, D. Liang, M. Zhou, F. Li, R. Li, J. Mater. Sci. 44 (24) (2009) 6736.